Available online at www.sciencedirect.com
ScienceDirect
Trans. Nonferrous Met. Soc. China 26(2016) 917−923
Transactions of Nonferrous Metals Society of China
www.tnmsc.cn

Wearing resistance of in-situ Al-based composites with different SiO_2/C/Al molar ratios fabricated by reaction hot pressing

El Oualid MOKHNACHE, Gui-song WANG, Lin GENG

School of Materials Science and Engineering, Harbin Institute of Technology, Harbin 150001, China

Received 21 April 2015; accepted 10 November 2015

Abstract: The in-situ Al-based composites with different SiO_2/C/Al molar ratios were fabricated by reaction hot pressing. The dry sliding wear characteristics of the composites were investigated using a pin-on-disc wear tester. Scanning electron microscopy (SEM) and energy dispersive X-ray spectroscopy (EDX) were used to investigate the surface composition and its morphology. The results show that when the SiO_2/C/Al molar ratio is 3:6:9, more in-situ synthesized Al_2O_3 and SiC along with Si particles are produced, and Al_4C_3 is prevented completely from the Al−SiO_2−C system. Thereby, a significant improvement of wear resistance is obtained. When the sliding velocity increases from 0.4 to 1.6 m/s, the wear loss decreases gradually. With increasing the normal load, the wear loss increases as well. Ploughing, craters and micro-grooving are observed as dominant abrasive wear mechanisms. Whereas, when a high velocity is employed, only the oxidation mechanism controls the wear behavior of the composites.
Key words: metal matrix composite; wear mechanism; friction; hardness

1 Introduction

Recently, the in-situ aluminum matrix composites (AMCs) have been applied widely as potential materials in automobile, aerospace and military applications due to their excellent properties such as specific strength, stiffness, wear resistance and elastic modulus [1−4]. Since AMCs have been used widely for tribological applications [1]. It is necessary to study the wear behavior of AMCs and further the improvement of wear properties. Indeed, many factors including the normal load, sliding velocity, type, orientation, size, shape and volume fraction of reinforcement should be pointed out to determine a unique information and many unexpected parameters can be produced [5]. Many ceramics such as Al_2O_3, SiC, Si and Al_4C_3 have been extensively employed as good wearing reinforcements [6−10]. These particles show excellent properties such as high melting temperature, high elastic modulus and high strength. However, the presence of hard Si and Al_4C_3 as brittle phases might also play a key role in determining the wear properties under specific conditions [11,12]. In our previous work [13], we investigated the reaction mechanisms in Al−SiO_2−C system, and we studied the effect of varying the SiO_2/C/Al molar ratio on the mechanical properties of the fabricated composites. It was found that when the SiO_2/C/Al molar ratio was 3:6:9, more in-situ Al_2O_3 and SiC along with Si particles formed, and Al_4C_3 was prevented completely from the SiO_2−C−Al system. In addition, a significant improvement of tensile properties was obtained. For further consideration, the wear properties have not yet been investigated. In this research, the influence of varying the SiO_2/C/Al molar ratio on the wear properties was investigated. Reactive sintering was used to produce three composites with different SiO_2/C/Al molar ratios of 3:0:9, 3:3:9 and 3:6:9. The influence of both the sliding velocity and normal load on the wear properties was studied as well.

2 Experimental

Pure aluminum powder (99.6% purity), silica powder (99.2% purity) and flaky carbon (99.8% purity) with average sizes of 30, 2 and 5 μm, respectively, were used as starting materials. The powder mixtures were ball-milled using low energy at 160 r/min for 4 h in a

Foundation item: Project (2012CB619600) supported by the Ministry of Science and Technology of China; Project (51201047) supported by the National Natural Science Foundation of China; Project (HIT.NSRIF.2013001) supported by the Fundamental Research Funds for the Central Universities, China; Project (20110491038) supported by the Postdoctoral Science Foundation of China
Corresponding author: Gui-song WANG; Tel: +86-451-86418674; Fax: +86-451-86413922; E-mail: wangguisong@hit.edu.cn
DOI: 10.1016/S1003-6326(16)64187-0

planetary ball mill under an argon atmosphere with a mass ratio of milled media to material of 4:1. The mixture powders were transferred into the graphic mold pre-coated with boron nitride to avoid the reaction between the mold and the reactants. Reaction hot pressing (RHP) was used to produce the composites namely S1, S2 and S3 with different SiO_2/C/Al molar ratios of 3:0:9, 3:3:9 and 6:3:9, respectively. In one step as shown in Fig. 1(a), the mixture of powders was heated from 25 to 600 °C and compacted with 25 MPa for 1 h. Then, the compact was heated to the synthesis temperature (1050 °C) and held for 1 h. Following which, the compact was cooled down to 580 °C and re-compacted with 25 MPa for 1 h to produce dense composites. The stoichiometric starting materials were weighed according to the hypothetical reactions shown in Table 1. The heating and cooling rates in all experiments were 10 °C/min. To prepare the wear samples, the tested wear surfaces of samples were polished to remove their oxidation surfaces. The dry sliding wear tests were conducted on a pin-on-disc wear testing machine at room temperature in the air atmosphere under a relative humidity of 30%−40%. The test pins are 9 mm in diameter and 15 mm in length. The counterpart discs were made of CGR15 steel with hardness of around HRC 62 and surface roughness (R_a) of 0.2 μm. The track radius was fixed to be 30 mm, as shown in Fig. 1(b).

The counterpart disc was 70 mm in diameter and 10 mm in thickness. The normal loads were 10, 20, 30 and 40 N separately for sliding velocities of 0.4, 0.8 and 1.6 m/s. An electronic balance with the precision of 0.001 mg was used to detect the mass loss. A scanning electron microscope (SEM, Quanta 200FEG) along with energy dispersive X-ray spectroscopy (EDX) was used to investigate the microstructures, morphologies and wear surfaces of the composites.

3 Results and discussion

3.1 Microstructures and mechanical properties

The SEM images of composites S1, S2 and S3 fabricated with different SiO_2/C/Al molar ratios of 3:0:9, 3:3:9 and 3:6:9 are shown in Figs. 2(a)−(c), respectively, which further confirm the presence of fine particles as reinforcements and their sizes are in order of micrometers.

Coupled with the XRD pattern of each composite (Fig. 3), in composite S1, only Al_2O_3 and Si are detected as new phases. Adding the carbon to the Al−SiO_2 system for composite S2, the XRD pattern confirms the presence of Al_2O_3, Si, Al_4C_3 and SiC. Additionally, when the SiO_2/C/Al molar ratio is 6:3:9, more Al_2O_3 and Si besides SiC form and Al_4C_3 is prevented completely from Al−SiO_2−C system.

Additionally, as shown in Figs. 4(a)−(c), TEM and EDX images show the presence of the rod-like Al_4C_3 (comprising of Al and C)), polygonal SiC (comprising of Si and C), polygonal Al_2O_3 (comprising of Al and O) and Si particles with sizes of around 0.4, 0.6, 1.8 and 0.3 μm, respectively. Also, it can be seen that there is no impurity existing at the interfaces between the reinforcements and aluminum matrix, indicating that the formed interface is

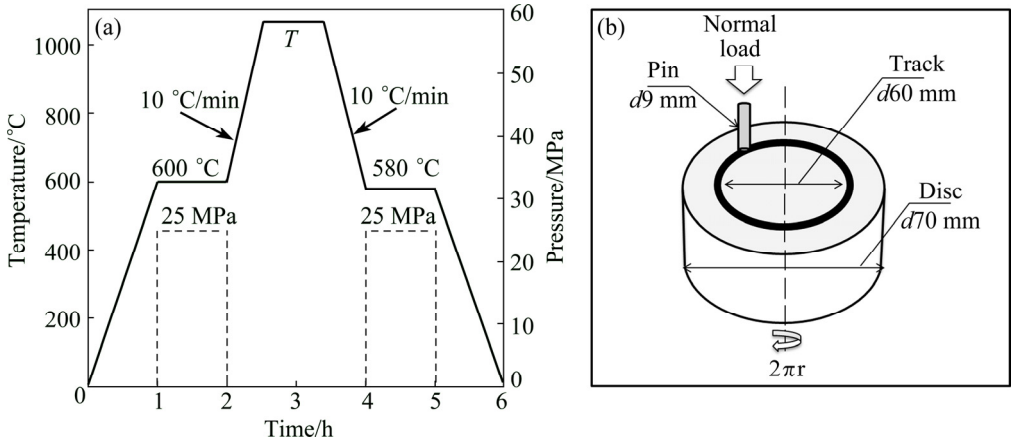

Fig. 1 RHP whole process (a) and pin-on-disc configuration (b)

Table 1 Composites nomenclature, hypothetical reactions, raw materials and produced phases

Composite	Hypothetical reaction	Mass of raw material/g			Produced phase
		Al	SiO_2	C	
S1	$3SiO_2+9Al→2Al_2O_3+3Si+5Al$	92.54	7.46	0.0	Al_2O_3, Si, Al
S2	$3SiO_2+9Al+3C→2Al_2O_3+3SiC+5Al$	91.29	7.25	1.46	Al_2O_3, SiC, Al
S3	$6SiO_2+9Al+3C→4Al_2O_3+3SiC+3Si+Al$	91.29	14.5	1.46	Al_2O_3, SiC, Si, Al

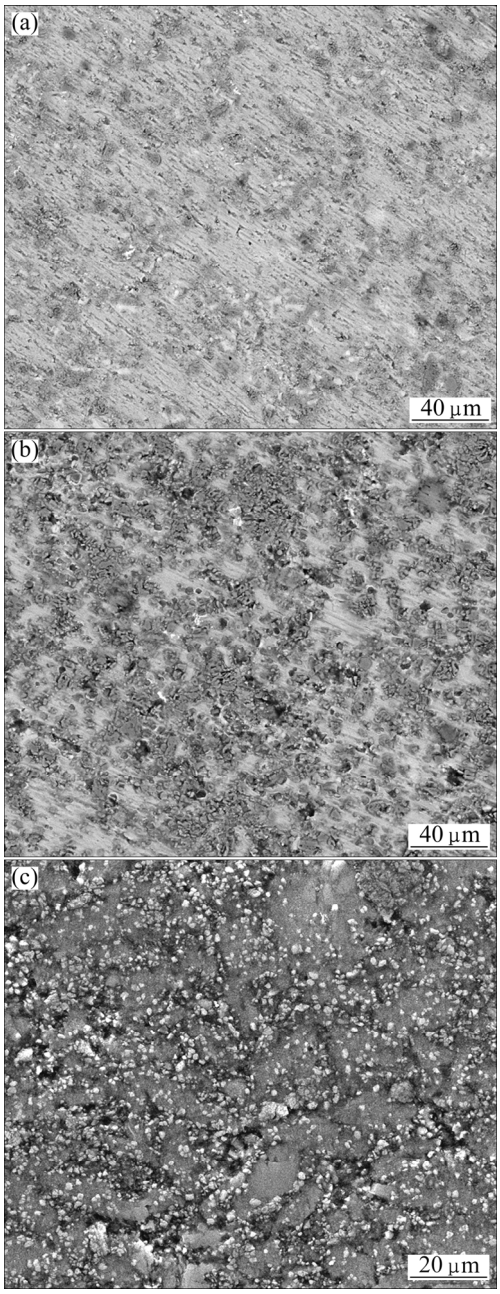

Fig. 2 SEM images of composites S1 (a), S2 (b) and S3 (c)

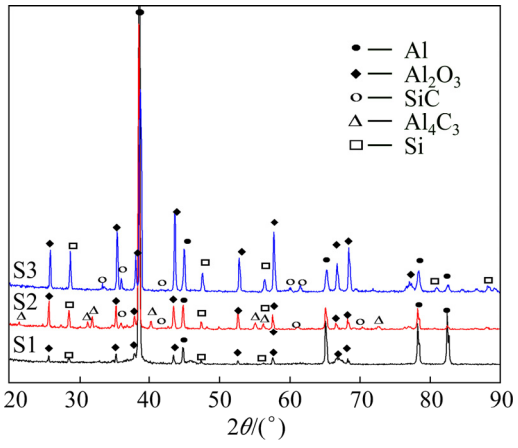

Fig. 3 XRD patterns of fabricated composites

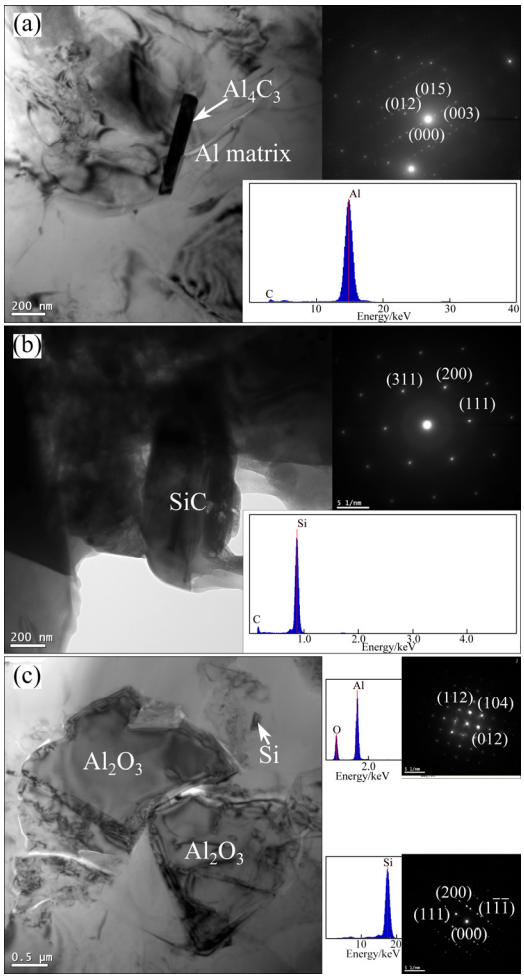

Fig. 4 TEM and EDX images of in-situ synthesized particles in Al−SiO_2−C system: (a) Al_4C_3; (b) SiC; (c) Al_2O_3 and Si

clean and free from any interfacial phase. These can be beneficial in improving the wear resistance of the composites. In fact, the advantage of using the ultrafine reinforcements in MMCs has been reported [1]. Accordingly, the in-situ methods promote a strong particles/matrix bonding. Moreover, these particles can be retained on the wear surface during sliding, and can increase the matrix resistance to indentation, thereby improving the wear resistance of MMCs.

The tensile properties and hardness of the composites S1, S2 and S3 are summarized in Table 2.

Table 2 Mechanical properties of fabricated composites S1, S2 and S3

Composite	Brinell hardness	Ultimate tensile strength/MPa	Yield strength/ MPa	Strain/ %
S1	45	121	59	12.4
S2	43.2	124	79	5.95
S3	56	161	138	2.3

3.2 Wear characteristics

As mentioned above, many factors including the kind, size distribution and volume of reinforcements, would affect the wear properties of the composites. Figure 5 shows the effect of the normal load at a sliding velocity of 0.8 m/s and sliding distance of 1000 m on the wear loss of the composites for different molar ratios. Obviously, when the load increases, all composites show the same wear behavior by increasing the wear loss. This is consistent with Archard's equation [14]. At the same time, the wear loss of composite S2 is somewhat lower than that of S1. This may be attributed to the formation of Al_4C_3 and SiC besides Al_2O_3 and Si as good bearing particles that resist to the material removal. In fact, Al_4C_3 is deleterious when it forms at the interface between SiC and Al matrix, but this phase can also be beneficial as strengthening particles in the AMCs [1]. Subsequently, when the SiO_2/C/Al molar ratio is 3:6:9, an improvement of wear resistance is obtained. This improvement is attributed to the formation of more in-situ synthesized Al_2O_3 and Si along with SiC. As reported by Ref. [15], the wear loss of materials is inversely proportional to its hardness which is the case in the present study. Therefore, in composite S3, its hardness (HB 56) is improved compared with those of S1 (HB 43.2) and S2 (HB 45), thereby increasing its wear resistance.

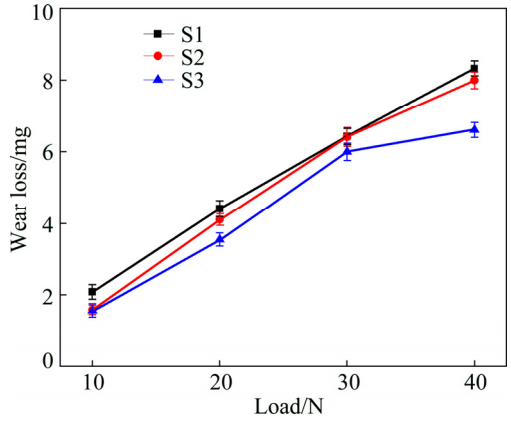

Fig. 5 Wear properties of composites S1, S2 and S3 at sliding velocity of 0.8 m/s vs normal load

Figure 6 shows the effect of sliding velocity on the wear loss at a normal load of 20 N for a sliding distance of 1000 m of the composites S1, S2 and S3. For each composite, the wear loss decreases with increasing the sliding velocity. During sliding tests, the main mechanisms for the reinforced composites that affect the wear resistance are work hardening and surface oxidation. As the work hardening layer can form firstly, the wear resistance will increase. However, the temperature also arises to a critical value that leads to the re-crystallization of the wear surface, thereby decreasing its hardness, which decreases the wear resistance. On the other hand, the oxidation layer can form due to the increase of temperature. In the present study, the wear loss decreases gradually with increasing the sliding velocity from 0.4 to 1.6 m/s. That is to say, only the oxidation mechanism is responsible for decreasing the wear loss of the composites. This phenomena is further confirmed in the next section.

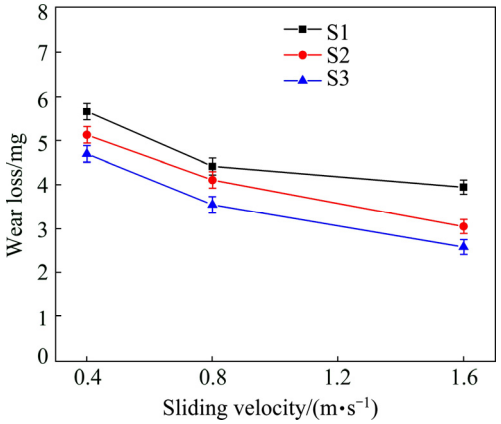

Fig. 6 Wear properties of composites S1, S2 and S3 at load of 20 N vs sliding velocity

3.3 Wear surfaces

Figures 7(a)−(c) show the SEM images of the worn surfaces of composites S1, S2 and S3 at a normal load of 20 N and a sliding velocity of 0.8 m/s, respectively. It can be seen clearly that the flow of the soft Al matrix was restricted due to the presence of the in-situ synthesized Al_2O_3, Si, Al_4C_3 and Si as second hard phases. As the formed interfaces between Al matrix and the in-situ synthesized particles are clean and free from any interfacial contamination, this would play a key role in improving the wear bearing capacity against the counterpart, thereby reducing the material removal. Typical surface damage like micro-grooves, micro-ploughing and craters are observed, crakes and fracture also exist when composite S3 was experienced to the high normal load (40 N). This can be attributed to the high content of the in-situ reinforcements when compared with composites S1 and S2. Cracks initiation, propagation and fracture are observed in the matrix near to hard reinforcements, due to increased stress concentration zones, as shown in Fig. 7(d). Moreover, the EDX result of the worn surface shows the presence of Fe (Fig. 7(e)) which is transferred from the counterpart. That is to say, the adhesive wear also exists during the sliding tests. The abrasive wear behavior of materials is generally controlled by material parameters in addition to the sliding conditions like normal load and abrasive medium [5]. Material loss under abrasive wear conditions is removed by ploughing and micro-cutting. These mechanisms require penetration by hard abrasive particles which in turn are controlled by the hardness of

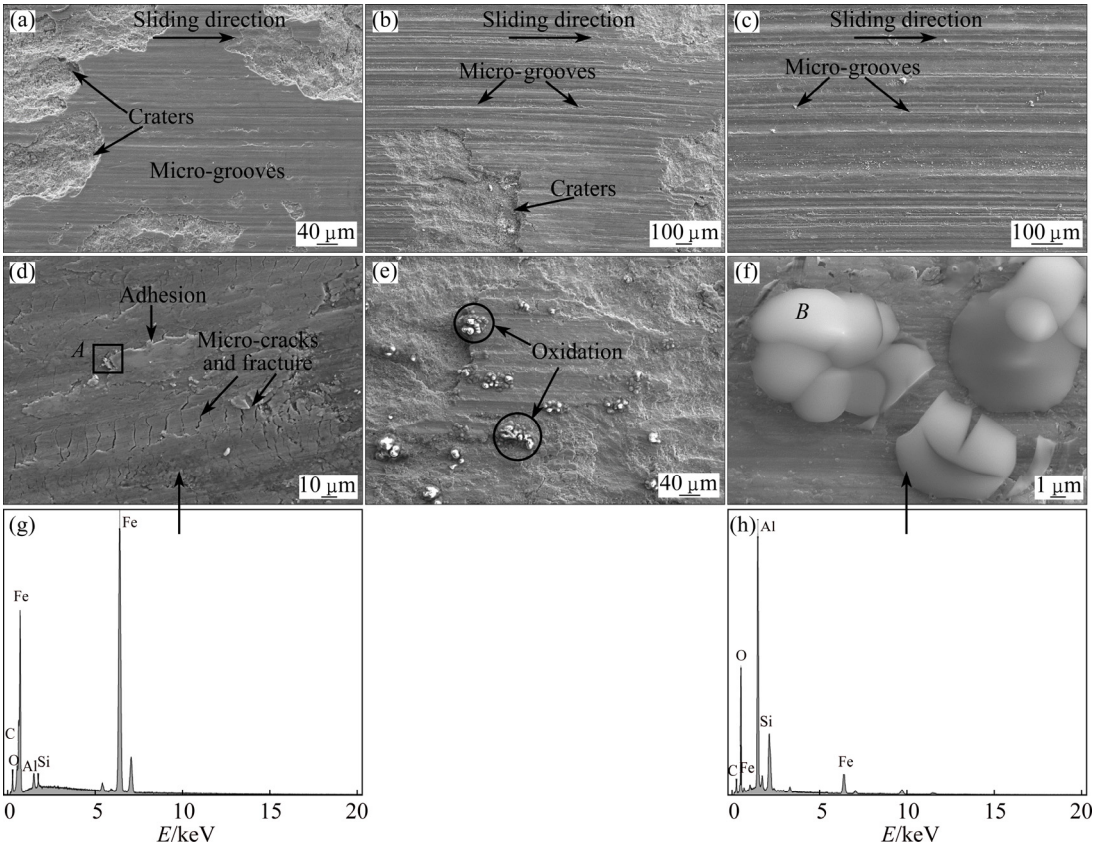

Fig. 7 SEM images of worn surfaces of composites S1 (a), S2 (b) and S3 (c) at load of 20 N and sliding velocity of 0.8 m/s and composite S3 at loads of 20 N (d) and 40 N (e, f) and sliding velocities of 0.8 m/s and 0.4 m/s, respectively; EDX analysis of square *A* in Fig. 7(d) (g) and point *B* in Fig. 7(f) (h)

material. Therefore, the hardness of the fabricated composites plays a significant role in controlling the wear loss during the sliding wear tests. In addition, large amounts of smooth particles form (Fig. 7(e)) as the sliding velocity increases. The EDX result confirms that these particles are Al_2O_3 oxides (comprising of Al and O as dominant elements), as shown in Fig. 7(h). This further confirms the above relationship between the wear loss and the sliding velocity. In other words, as the velocity increases, the wear loss is controlled by the oxidation mechanism.

Figures 8(a)−(c) show the SEM images of wear debris formed in composite S3 at different normal loads and a sliding velocity of 0.8 m/s for a sliding distance of 1000 m. Various shapes and sizes of wear debris are found as a result of the dry sliding test. In agreement with the previous researches [16,17], the shape of wear debris varies from fine particles to coarse flakes and platelet forms. The EDX results show that this debris is constituted of Fe, Al, O, C and Si as predominant elements, as shown in Fig. 8. The presence of Fe may have derived in transfer from the sliding steel disc. The element O is considered to have arisen in reactions with the environment, indicating that the mode of wear is mildly oxidative [18].

3.4 Friction coefficients

The friction mainly depends on the material properties such as hardness, strain, density, shear strength, modulus of elasticity, yield and ultimate tensile strength [19]. Figure 9(a) shows the variation in friction coefficient (μ) of composites S1, S2 and S3 at a normal load of 20 N and a sliding velocity of 1.6 m/s for a sliding distance of 1000 m. Evidently, it seems that varying the SiO_2/C/Al molar ratio from 3:0:9 to 3:3:9 does not affect the friction coefficient much. As the employed volume fraction of reinforcements in composites S1 and S2 is the same (10%), and only the kind of reinforcement is different where both the SiC and Al_4C_3 particles are present in composite S2, this may explain the slight reduction of friction coefficient. However, when the SiO_2/C/Al molar ratio of 3:6:9 was used, high contents of Al_2O_3 and Si besides SiC were produced, thereby reducing the contact area between the composite and counterpart. As a result, the friction coefficient decreases from 0.6738 to 0.5334 systematically.

Figure 9(b) shows the variation in friction

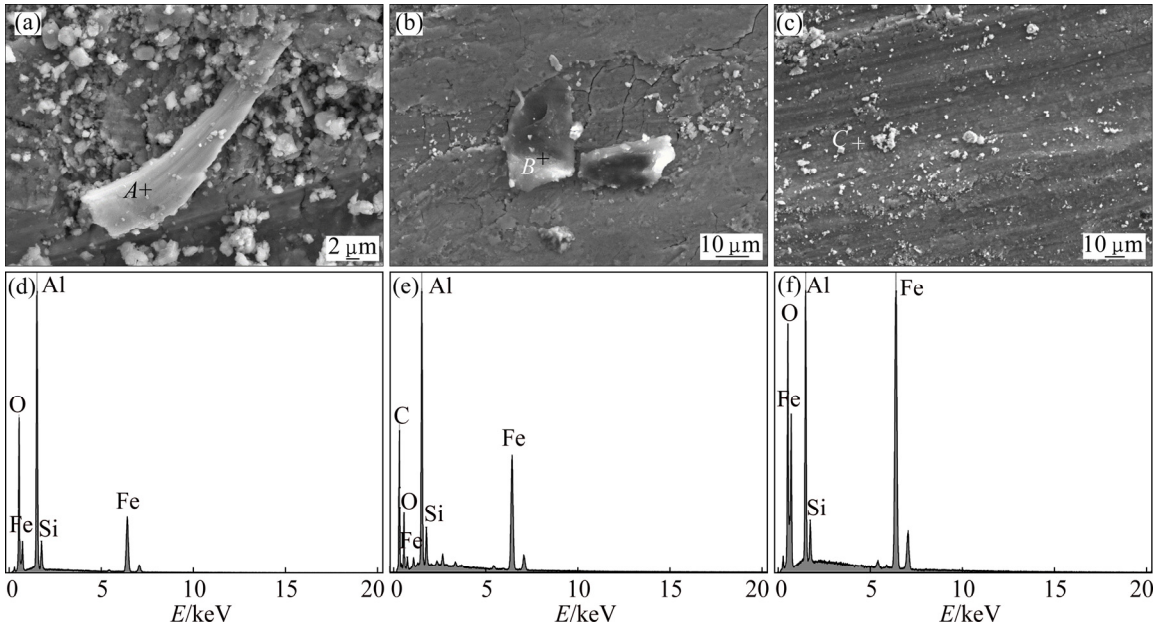

Fig. 8 SEM images (a−c) and EDX analysis (d−f) of wear debris formed in composite S3 at sliding velocity of 0.8 m/s and loads of 10 N (a, b, d, e) and 40 N (c, f)

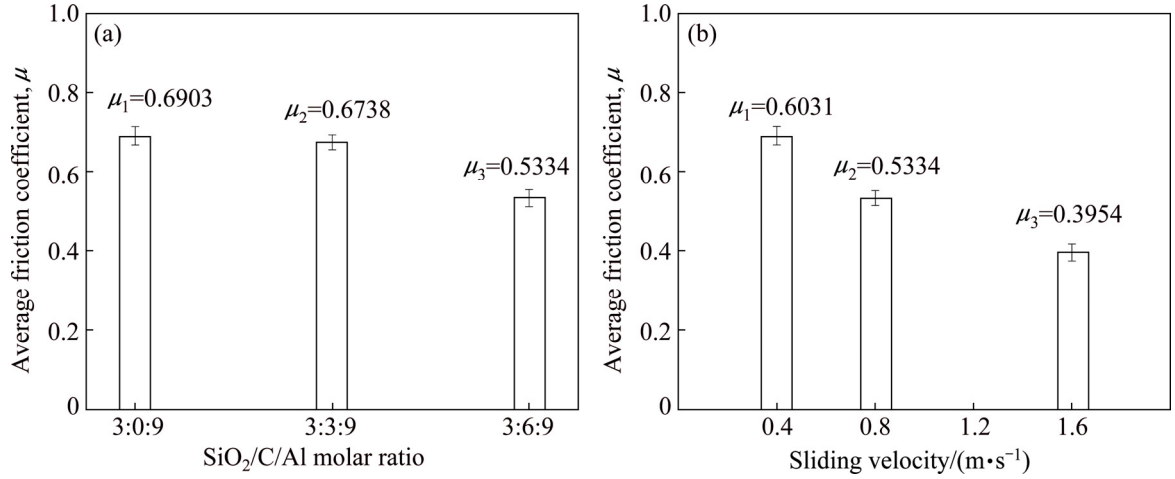

Fig. 9 Average friction coefficient vs variation of SiO_2/C/Al molar ratio (a) and sliding velocity (b)

coefficient (μ) of composite S3 as a function of the sliding velocity at a normal load of 20 N for a sliding distance of 1000 m. Obviously, when the velocity increases from 0.4 to 1.6 m/s, the friction coefficient reduces significantly. This is because, the contact time changes from 1250 to 625 s and both the adhesion and deformation forces needed to plow out the particles on the surfaces decrease. Thereby, the friction coefficient decreases from μ_1=0.6031 to μ_3=0.3954. Moreover, Al_2O_3 oxides that formed at high sliding velocity as third abrasion body (Fig. 7(e)) also contribute to the reduction of the friction coefficient of composite S3.

4 Conclusions

1) When the SiO_2/C/Al molar ratio is 3:6:9, more in-situ synthesized Al_2O_3 and SiC along with Si particles are produced, and Al_4C_3 is prevented completely from the Al−SiO_2−C system. Thereby, a significant improvement of wear resistance is obtained.

2) The wear loss of the composites increases with increasing the load. However, when the sliding velocity increases, the wear loss decreases systematically.

3) Ploughing, micro-grooving and craters are observed as dominant wear mechanisms. Whereas, the oxidation mechanism controlls the wear loss when the sliding velocity increases.

4) When the velocity increases, the friction coefficient decreases owing to the formation of smooth Al_2O_3 oxides as third abrasion body.

5) The friction coefficient decreases from 0.6738 to 0.5334 when the SiO_2/C/Al molar ratio varies from 3:0:9 to 3:6:9.

References

[1] TJONG S C, MA Z Y. Microstructural and mechanical characteristic of in situ metal matrix composites [J]. Materials Science and Engineering R, 2000, 29(3−4): 49−113.

[2] ROSENBERGER M R, FORLERER E, SCHVEZOV C E. Wear behavior of AA1060 reinforced with alumina under different loads [J]. Wear, 2009, 266(1−2): 356−359.

[3] JIMÉNEZ A E, BERMÚDEZ M D, CINTAS J, HERRERA E J. Dry wear of $NiAl_3$-reinforced mechanically alloyed aluminum with different microstructure [J]. Wear, 2009, 266(1−2): 255−265.

[4] ZHU H G, WANG H Z, GE L Q, XU W J, YUAN Y Z. Study of the microstructure and mechanical properties of composites fabricated by the reaction method in an Al−TiO_2−B_2O_3 system [J]. Materials Science and Engineering A, 2008, 478(1−2): 87−92.

[5] SANNINO A P, RACK H J. Dry sliding wear of discontinuously reinforced aluminum composites: Review and discussion [J]. Wear, 1995, 189(1−2): 1−19.

[6] JIANG Xiao-song, WANG Nai-juan, ZHU De-gui. Friction and wear properties of in-situ synthesized Al_2O_3 reinforced aluminum composites [J]. Transactions of Nonferrous Metals Society of China, 2014, 24(7): 2352−2358.

[7] WALCZAK M, PIENIAK D, ZWIERZCHOWSKI M. The tribological characteristics of SiC particle reinforced aluminium composites [J]. Archives of Civil and Mechanical Engineering, 2015, 15(1): 116−123.

[8] MIYAJIMA T, IWAI Y. Effects of reinforcements on sliding wear behavior of aluminum matrix composites [J]. Wear, 2003, 255(1−6): 606−616.

[9] DEUIS R L, SUBRAMANIAN C, YELLUP J M. Dry sliding wear of aluminium composites—A review [J]. Composites Science and Technology, 1997, 57(4): 415−435.

[10] ARIK H, OZCATALBAS Y, TURKER M. Dry sliding wear behavior of in situ Al−Al_4C_3 metal matrix composite produced by mechanical alloying technique [J]. Materials and Design, 2006, 27(9): 799−804.

[11] MOKHNACHE E O, WANG G S, GENG L, HUANG L J. Microstructures and mechanical properties of in situ Al_2O_3/Al−Si composites fabricated by reaction hot pressing [J]. Metallurgical and Materials Transactions B, 2014, 45(6): 1965−1969.

[12] VIALA J C, BOSSELET F, LAURENT V, LEPETITCORPS Y. Mechanism and kinetics of the chemical interaction between liquid aluminium and silicon carbide single crystals [J]. Journal of Materials Science, 1993, 28(19): 5301−5312.

[13] MOKHNACHE E O, WANG G S, GENG L, KAVEENDRAN B, HENNICHE A, RAMDANI N. In situ Al based composites fabricated in Al−SiO_2−C system by reaction sintering [J]. JOM: The Journal of The Minerals, Metals & Materials Society (TMS), 2015, 67(7): 1505−1514.

[14] PURCEK G, SAVASKAN T, KUCUKOMEROGLU T, MURPHY S. Dry sliding friction and wear properties of zinc-based alloys [J]. Wear, 2002, 252(11−12): 894−901.

[15] SAVASKAN T, HEKIMOĞLU A P, PÜRCEK G. Effect of copper content on the mechanical and sliding wear properties of monotectoid-based zinc−aluminium−copper alloys [J]. Tribology International, 2004, 37(1): 45−50.

[16] SHAH K B, KUMAR S, DWIVEDI D K. Aging temperature and abrasive wear behaviour of cast Al−(4%, 12%, 20%)Si−0.3%Mg alloys [J]. Materials and Design, 2007, 28(6): 1968−1974.

[17] GHAZALI M J, RAINFORTH W M, JONES H. The wear of wrought aluminium alloys under dry sliding condition [J]. Tribology International, 2007, 40(2): 160−169.

[18] DWIVEDI D K. Microstructure and dry sliding wear behaviour of cast Al−8%Si−0.3%Mg alloy against En-31[J]. ISIJ International, 2006, 46(7): 1101−1105.

[19] DWIVEDI D K, ARJUN T S, THAKUR P, VAIDYA H, SINGH K. Sliding wear and friction behaviour of Al−18%Si−0.5%Mg alloy [J]. Journal of Materials Processing Technology, 2004, 152(3): 323−328.

反应热压制备不同 SiO_2/C/Al 摩尔比原位自生铝基复合材料的耐磨性能

El Oualid MOKHNACHE，王桂松，耿 林

哈尔滨工业大学 材料科学与工程学院，哈尔滨 150001

摘 要：反应热压法制备不同 SiO_2/C/Al 摩尔比的原位自生铝基复合材料。采用销−盘式摩擦试验机对这些复合材料进行干滑动摩擦试验。利用扫描电镜和能谱分析研究复合材料表面成分和形貌。结果表明，当 SiO_2/C/Al 摩尔比为 3:6:9 时，原位生成更多 Al_2O_3、SiC 和 Si 颗粒，在 Al−SiO_2−C 体系中 Al_4C_3 相被彻底抑制，因此复合材料的耐磨性能大幅度提高。当滑动速度从 0.4 m/s 增加到 1.6 m/s 时，磨损量逐渐减小。当摩擦载荷增加时，磨损量也增加。观察到的犁沟、磨损坑和细微纹沟说明磨料磨损是主要的磨损机制。然而，当采用更高的滑动速度时，只有氧化磨损机制控制复合材料的磨损行为。

关键词：金属基复合材料；磨损机制；摩擦；硬度

(Edited by Mu-lan QIN)